Interaction and Dimerization Energies in Methyl-Blocked α,γ-Peptide Nanotube Segments

Rebeca García-Fandiño,[†,‡] Luis Castedo,[†] Juan R. Granja,*[,†] and Saulo A. Vázquez*[,§]

Departamento de Química Orgánica, Universidad de Santiago de Compostela, 15782 Santiago de Compostela, Spain, Departamento de Química Fundamental, Facultad de Ciencias, Universidad de A Coruña, 15071 A Coruña, Spain, and Departamento de Química Física, Universidad de Santiago de Compostela, 15782 Santiago de Compostela, Spain

Received: November 17, 2009; Revised Manuscript Received: March 11, 2010

The building blocks of a promising class of peptide nanotubes composed of alternating *D*-α-amino acids and (1*R*,3*S*)-3-aminocyclohexane (or cyclopentane) carboxylic acid (*D*-γ-Ach or *D*-γ-Acp) were explored by computational methods. Specifically, density functional theory (DFT) calculations on monomers and dimers of γ-Ach-based and γ-Acp-based α,γ-cyclo-hexapeptides and cyclo-octapeptides were carried out to investigate the experimentally observed preference for α−α over γ−γ dimerization, associated with the two types of stacking patterns present in these peptide nanotubes, as well as the preference for heterodimerization versus homodimerization. Full geometry optimizations were performed at the B3LYP/6-31G(d) level, and single point calculations were subsequently carried out with the B3LYP and M05-2X functionals and the 6-31+G(d,p) basis set. The calculations predict that the interaction energies in the α−α species are quite similar to those in the γ−γ dimers. However, a comparison of dimerization energies (i.e., interaction energies plus deformation energies of monomers) shows that α−α dimerization is energetically favored over γ−γ dimerization. The calculations strongly suggest that the preference for α−α binding is governed by differences between the deformation energies in the α and γ monomers, rather than by differences between the relative strengths of the α−α and γ−γ hydrogen-bonding patterns. Calculations based on local properties of the electron density support the previous suggestion that the H−N bonds of the α-amino acids are more polarized than those of the γ-amino acids.

I. Introduction

Over the last years, many researchers have directed their attention toward the field of nanoscience and nanotechnology, with the aim of contributing to the development of potentially important technologies, and with the help of powerful experimental techniques (e.g., scanning probe microscopy) for observing and manipulating materials at the atomic and molecular level. The design of new synthetic methods has allowed the preparation of uniform nanostructures of a wide variety of compositions and shapes. Examples are nanotubes,[1–5] nanowires,[5–9] block copolymers,[10,11] nanocrystals,[12] and self-assembled monolayers.[13] The chemistry of nanotubes started with the discovery of carbon nanotubes by Iijima[1] in 1991, and soon it was extended to other hollow tubular structures of inorganic and organic nature. In particular, self-assembling peptide nanotubes (SPNs) have been extensively studied due to their potential applications in chemistry, biology, and material science.[4] The first peptide nanotubes derived from cyclic peptides (CPs) were reported in 1993 by Ghadiri and were based on alternating *D* and *L* α-amino acids.[14,15] Since then, other types of peptide nanotubes have been synthesized using different amino acids,[15–22] including the α,γ-SPNs that consist of alternating 3-aminocycloalkanecarboxylic acid (γ-Aca), such as (1*R*,3*S*)-3-aminocyclohexanecarboxylic acid (*D*-γ-Ach) or (1*R*,3*S*)-3-aminocyclopentanecarboxylic acid (*D*-γ-Acp) and α-amino acid (see Figure 1).[23–29] All of the SPNs are prepared from cyclic peptide rings stacked on top of each other via hydrogen bonds formed between C═O and NH groups located in adjacent rings, leading to β-sheet-like tubular structures.[14,30]

One of the advantages of SPNs is the ease with which these materials can be made and modified. Particularly, the pore size of SPNs is controlled by the size of the CPs. SPNs with large pore diameters are, however, difficult to synthesize because large peptide rings tend to adopt folded conformations, which prevents CP stacking.[31,32] In this respect, especially interesting are those derived from α,γ-CPs that allow the preparation of ensembles with large pore diameters (up to 15 Å) due to the rigidity and flatness induced by the cycloalkane segments.[23] Moreover, while almost all the cyclic peptide nanotubes that have been prepared so far have hydrophilic inner surfaces and can permeate polar molecules only,[33–35] in the case of the α,γ-SPNs, the C2 methylene group of each cycloalkane moiety is projected into the lumen of the cavity, generating a partially hydrophobic cavity, which can be modulated by simple chemical modification of the β-carbon of the cycloalkane moiety of γ-Acas,[36] thus allowing, in principle, the fine control of the transport properties of a very wide range of molecules in the nanotube.[37]

The SPNs prepared from α,γ-CPs present, as shown graphically in Figure 1, two types of β-sheet-like hydrogen-bonding interactions: one connects the C═O and NH groups of the γ-amino acid (marked as γ−γ in the figure), and the other involves those of the α-amino acid (α−α interaction). Experimental work on hexameric and octameric γ-Ach-based and γ-Acp-based α,γ-CPs led to the suggestion that α−α bonding is stronger than γ−γ bonding. The experiments were conducted with *N*-methylated CPs, as specified in Figure 1, leading to two different classes of dimers, characterized by α−α or γ−γ H-bonding patters.[24–26] For example, at 298 K, *c*-[(*L*-γ-Ach-*D*-

* To whom correspondence should be addressed. E-mail: juanr.granja@usc.es (J.R.G.); saulo.vazquez@usc.es (S.A.V.).

† Departamento de Química Orgánica, Universidad de Santiago de Compostela.

‡ Universidad de A Coruña.

§ Departamento de Química Física, Universidad de Santiago de Compostela.

10.1021/jp910919k
Published on Web 03/30/2010

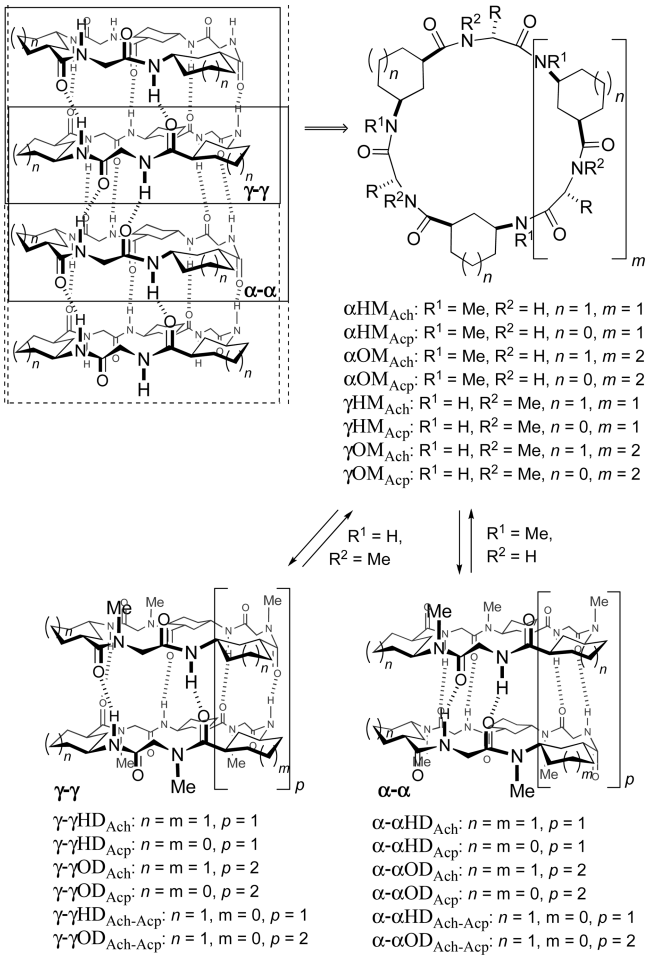

Figure 1. Schematic drawing for self-assembling peptide nanotubes composed of *c*-[(*L*-^{Me}*N*-γ-Ach-*D*-Ala)$_{3,4}$-] or *cyclo*-[(*L*-γ-Acp-*D*-^{Me}*N*-Ala)$_{3,4}$-] units, involving the α−α and γ−γ hydrogen-bonding patterns.

^{Me}*N*-Ala)$_3$-] forms γ−γ hexapeptide dimers, with an association constant of 230 M^{-1} in $CDCl_3$ and 2.5×10^4 M^{-1} in 2:3 $CDCl_3$/CCl_4.[27] The association constant for dimerization of *c*-[(*D*-Phe-*L*-^{Me}*N*-γ-Ach)$_3$-], that is, for formation of α−α hexapeptide dimers, was estimated to be 10^6 M^{-1} in chloroform.[28] The difference in stabilities between the α−α and γ−γ dimers was interpreted as the result of three contributions: (1) different backbone conformations, with the α−α conformation being better fitted than the γ−γ conformation, (2) a larger polarization of the NH group of the α-amino acid, relative to that of the γ-amino acid,[26] and (3) to steric interactions between the *N*-methyl and carbonyl groups on the α-face, which might prevent the CP from adopting a conformation as flat as is required for strong dimerization in β-strand form (effects of this kind have been observed in experimental and computational studies of β-conformations of model peptides).[29,38,39]

Besides the construction of SPNs by homodimeric units, we have showed, by studies with the N-methylated peptides, that heterodimerization between γ-Ach-based and γ-Acp-based α,γ-CPs is not only possible but is favored over homodimerization.[25] Specifically, addition of γ-Acp-based α,γ-CPs to a solution of γ-Ach-based α,γ-CPs leads almost exclusively to α−α heterodimerization; that is, γ-Acp-based α,γ-CPs stack with γ-Ach-based α,γ-CPs. This strong preference for heterodimerization is independent of the α-Aa side chains and the origin of this selectivity is unclear, although it was suggested, based on the X-ray data, that the heterodimer is more stable because of an improved alignment of hydrogen-bond donors and acceptors.[25] These homo- and heterodimerization equilibriums are quite common in nature and constitute an economical means toward structural diversity and functional versatility that potentially extend the benefits of this supramolecular process. The supramolecular advantage of heterodimerization versus homodimerization, together with its independence with the α-Aa side chains, has been used advantageously in electron and energy transfer processes using Acp- and Ach-based CPs decorated with appropriate donor and acceptor moieties.[28,40]

Computational simulations of cyclic peptides and peptide nanotubes[37,41–65] constitute a valuable complement to the experimental investigations and may provide further insights into the structural properties of these compounds. In fact, in early 1974, a theoretical analysis of conformations by Santis and co-workers[66] led them to predict the possibility of the formation of β-sheet-like tubular structures held together by both van der Waals and hydrogen bonds between C═O and NH groups. The calculation of equilibrium structures and interaction energies between CPs in dimers and oligomers has been undertaken in several studies. Gailer and Feigel[41] performed semiempirical AM1 calculations to investigate the geometry and energy of parallel and antiparallel peptidic β-sheets, and predicted a small enthalpy difference between the two arrangements and a stabilization energy per hydrogen bond of about −4.3 kcal/mol (assuming that all the interaction energy between monomers is associated with hydrogen bonding). Later, AM1 calculations on monomers and dimers of *c*-[(*L*-Phe^1-*D*-Ala^2)$_n$-] (n = 3−6), and density functional theory (DFT) calculations on the species with $n = 4$, showed that the antiparallel stacking scheme is favored over the parallel one,[46] in agreement with previous solution studies.[67] The DFT calculations, using the B3LYP functional, afforded interaction energies of about −5.7 kcal/mol for each hydrogen bond. This value is similar to those calculated for a *cyclo*-β-tetrapeptidedimer using three different functionals.[50] Lewis and co-workers[42] investigated the cyclic peptide system *c*-[(*D*-Ala-*L*-Glu-*D*-Ala-*L*-Gln)$_{m=1-4}$-] with a theoretical method, proposed for molecular dynamics simulations, in which the strong intramolecular interactions are handled with DFT and the weak intermolecular interactions (e.g., hydrogen bonds) are treated with a simple theory that accounts for Coulombic, exchange, and hopping interactions between the weakly interacting fragments. For *c*-[(*D*-Ala-*L*-Glu-*D*-Ala-*L*-Gln)$_2$-], they predicted a binding energy per dimer of 58.6 kcal/mol, which gives an interaction energy of −7.3 kcal/mol for each hydrogen bond. Tan et al.[47] carried out B3LYP/3-21G calculations to study the energetic and structural characteristics of *c*-[(β^3-HGly)$_4$-] and its oligomers (up to the ninomer). They found that the average interaction energy between two adjacent monomers in the *cyclo*-β-peptide oligomers increases significantly (in absolute value) upon addition of more monomers. The enhancement decreases gradually with the number of monomers, until eventually there would be no net increase upon addition of more units, thus yielding a stable SPN.

The present computational study was designed to complement the experimental work on hexameric and octameric γ-Ach-based and γ-Acp-based α,γ CPs,[24–26,28] and, more specifically, to investigate the origin of the large difference in association constants for both types of interaction, as well as the observed preference for heterodimerization. For this purpose, we selected the model systems depicted in Figure 1, in which the side chains are considered to be methyl groups. In this regard, it is important to remark that the experimental work shows that the above trends are not influenced by the nature of the side chains.[25]

Because of the size of these systems, the use of accurate correlated wave function theory is unfeasible with the present computational resources. As an alternative, we employed two different DFT functionals; one was the most popular up-to-date functional, namely, B3LYP,[68–70] and the other was M05-2X, which is one of the functionals proposed by Truhlar and co-workers for calculating noncovalent interaction energies in large biological systems.[71,72]

II. Computational Methods

As already mentioned, the present DFT calculations were conducted with the B3LYP and M05-2X methods. The former combines Becke's three-parameter nonlocal hybrid exchange potential[68,69] with the nonlocal correlation functional of Lee, Yang, and Parr.[70] It is well-known that this functional fails to correctly describe dispersion interactions. M05-2X[71,72] is one of the new generation DFT methods based on simultaneously optimized exchange and correlation functionals that include kinetic energy density in both functionals. This functional gives good performance for a benchmark database of 22 noncovalent complexes, including both hydrogen-bonding and dispersion-dominated complexes.[72,73] Full geometry optimizations (with no geometry constraints) were carried out with the B3LYP method and the standard 6-31G(d) basis set.[74] The starting geometries of the cyclic peptide dimers investigated in this work were constructed from X-ray crystallographic data of related compounds: *c*-[(*D*-^{Me}*N*-Ala-*L*-γ-Ach)$_4$-], *c*-[(*D*-Phe-*L*-^{Me}*N*-γ-Ach)$_3$-], *c*-[(*D*-Phe-*L*-^{Me}*N*-γ-Ach)$_4$-], and *c*-[(*D*-Leu-*L*-^{Me}*N*-γ-Acp)$_4$-].[23,24,26] The optimized geometries were subsequently used to obtain more accurate energies by single point calculations with the B3LYP and M05-2X functionals, in conjunction with the 6-31+G(d,p) basis set,[74] recommended by Truhlar and co-workers.[71,72] We notice that the M05-2X method showed relatively slow SCF convergence, and for this reason, we only used B3LYP for geometry optimizations. All of the DFT calculations reported in this study were performed with the Gaussian 03 package.[75]

Interaction energies were evaluated as the difference between the electronic energy of the dimer and the sum of the electronic energies of the separated monomers, with the same geometries as they have in the dimer (i.e., frozen geometries). The monomer energies were corrected for basis set superposition error (BSSE), using the counterpoise approach.[76,77] Dimerization energies were calculated as the energies of the dimers minus the energies of the separated and optimized monomers. The difference between the dimerization energy and the interaction energy is the deformation energy of the monomers (the geometry of an isolated monomer changes, in general, upon complex formation).

As a first approach, the starting geometries for the optimizations of the monomers were taken from the geometries of the optimized dimers. However, this approximation would ignore other possible conformations adopted by the single monomers. To overcome this limitation, we carried out molecular dynamics (MD) simulations of the monomeric units with the Gromacs 4.0 software package.[78] The atomic coordinates used in the MD simulations were taken from the corresponding DFT minimized structures of the monomers, and they were solvated with a chloroform box. The GAFF force field[79,80] was used for the cyclopeptide, and the Kollman model[81,82] was taken for chloroform. In general, the systems were simulated for 10 ns (with a time step of 2 fs) at constant volume and temperature (300 K) using the Berendsen thermal coupling and the energies and coordinates were saved every 2 ps. The LINCS algorithm[83] was employed to remove bond vibrations, and the particle mesh Ewald method,[84] to treat the long-range electrostatics. Periodic boundary conditions were applied in all three directions of space.

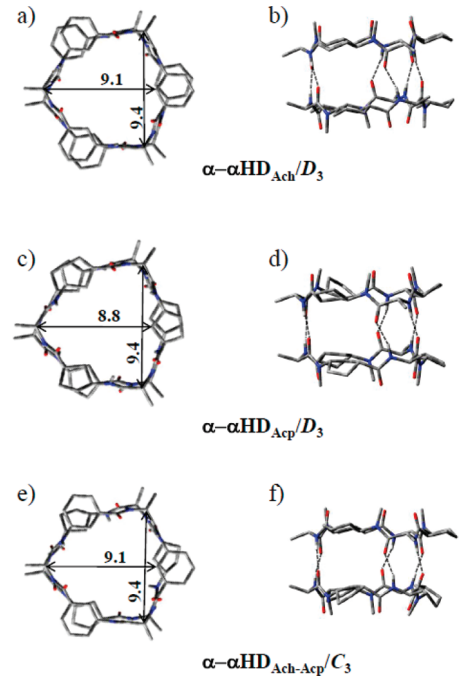

Figure 2. Conformations of α−α hexapeptide dimers optimized at the B3LYP/6-31G(d) level, as viewed along (a, c, and e) or perpendicular to (b, d, and f) the dimer axis. The approximate symmetry is indicated. Values for selected interatomic distances are given in Å.

Electron densities obtained at the B3LYP/6-31+G(d,p) level were analyzed by means of the quantum theory of atoms in molecules (QTAIM)[85,86] in order to assess relative strengths of the O···H(N) hydrogen bonds. In the QTAIM approach, the chemical bonding of a system is characterized by the topology of the electron density $\rho(\mathbf{r})$. When two atoms are bonded to each other, their nuclei are linked by a line of maximum ρ, called the bond path, and there is a surface defining their mutual boundary which intersects this line at the point where the density (along this line) is minimum. At this point of the bond path, the density gradient, $\nabla\rho$, is zero and two of the eigenvalues of the Hessian matrix of the density are negative (those associated with the directions perpendicular to the bond path), while the other eigenvalue is positive. This point is referred to as a (3,−1) bond critical point (BCP). Several local properties were evaluated at the BCPs of the O···H−N moieties, namely, the electron density, ρ_b, its Laplacian, $\nabla^2\rho_b$, and the local energy density, H_b. The QTAIM calculations were performed with the AIMPAC program.[87,88]

III. Results and Discussion

A. Conformations. The nomenclature employed to name the structures investigated in this work is given in Figure 1. A capital letter, O or H, is used to designate octapeptide or hexapeptide, respectively; it is followed by a second (capital) letter that indicates whether the compound is a monomer (M) or a dimer (D). Greek letters (α, γ) are added to specify whether the N−H bonds are in the α or γ amino acids. For example, αHM refers to hexapeptide monomers with N−H bonds located in the α amino acids; α−αHD denotes hexapeptide dimers in which the N−H units belong to α amino acids, giving rise to α−α stacking via hydrogen-bonding interactions with the O=C counterparts. Finally, a subscript, Ach or Acp, is included to refer to γ-Ach or γ-Acp amino acids, respectively. Heterodimers are named using the subscript Ach−Acp.

Figures 2−5 depict the geometries of the dimers optimized in this study (Cartesian coordinates of all the optimized

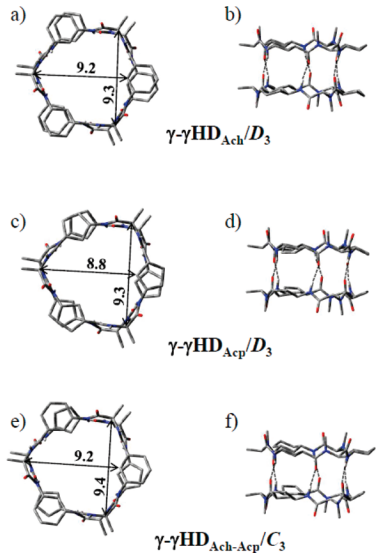

Figure 3. Conformations of $\gamma-\gamma$ hexapeptide dimers optimized at the B3LYP/6-31G(d) level, as viewed along (a, c, and e) or perpendicular to (b, d, and f) the dimer axis. The approximate symmetry is indicated. Values for selected interatomic distances are given in Å.

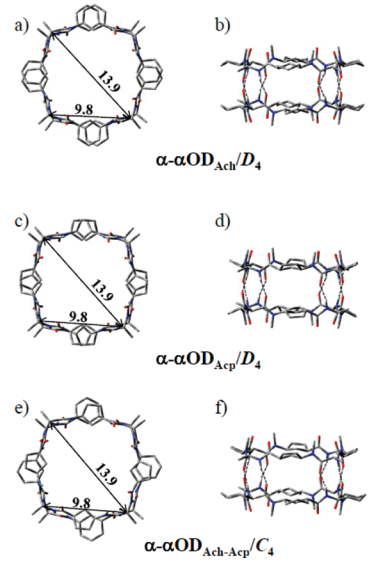

Figure 4. Conformations of $\alpha-\alpha$ octapeptide dimers optimized at the B3LYP/6-31G(d) level, as viewed along (a, c, and e) or perpendicular to (b, d, and f) the dimer axis. The approximate symmetry is indicated. Values for selected interatomic distances are given in Å.

structures are available in the Supporting Information). For clarity, hydrogen atoms other than those intervening in hydrogen bonding are not shown. The shapes of the hexameric dimers (Figures 2 and 3) are roughly triangular. Homodimers HD$_{Ach}$ and HD$_{Acp}$ (with either $\alpha-\alpha$ or $\gamma-\gamma$ bonding) have approximately D_3 symmetry, and heterodimers HD$_{Ach-Acp}$ show C_3 symmetry. As mentioned in the preceding section, no symmetry constraints were imposed in the geometry optimizations. Therefore, deviations from exact symmetry in the calculated structures may arise from the geometry optimization procedure, which, in floppy systems, may lead to a point relatively away from the exact minimum. Because of this, in some cases, the values indicated in the figures correspond to averages of equivalent interatomic distances. In general, the ODs (Figures 4 and 5) exhibit square shapes, and have almost D_4 symmetry ($\alpha-\alpha$ homodimers) or C_4 symmetry ($\alpha-\alpha$ heterodimer). The $\gamma-\gamma$ODs, however, have essentially D_2 symmetry (homodimers) or C_2 symmetry (heterodimer).

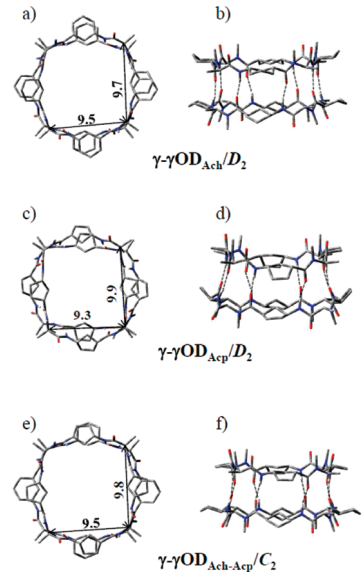

Figure 5. Conformations of $\gamma-\gamma$ octapeptide dimers optimized at the B3LYP/6-31G(d) level, as viewed along (a, c, and e) or perpendicular to (b, d, and f) the dimer axis. The approximate symmetry is indicated. Values for selected interatomic distances are given in Å.

The views from the sides (drawings b, d, and f in Figures 2−5) show, in most cases, flat rings with the C═O and NH groups oriented roughly perpendicular to the ring planes. The $\gamma-\gamma$ODs, however, show a slight deviation from ring planarity, which, to a certain degree, may be caused by steric interactions between the *N*-methyl and carbonyl groups, as mentioned in the Introduction. When the optimized structures of the hexameric and octameric dimers are viewed along the axes (views a, c, and e in Figures 2−5), it is apparent that one of the monomers is slightly rotated with respect to the other. This feature has also been observed in the crystallographic structures of hexapeptide and octapeptide dimers.[24−26] The reason for this effect may be attributed, to a large extent, to the geometrical characteristic of C═O···HN hydrogen bonds, which should be most favorable for C═O···H angles around 120° due to the directionality of the oxygen lone pairs. Also, steric repulsions may play some role in the conformations of these compounds.

The largest distances between backbone atoms belonging to the same monomer (excluding the most distant atoms of the Ach and Acp rings) are ≈9 Å in the HDs and ≈14 Å in the OD structures. The distances between rings in the dimers, listed in Table 1, are about 4.8−5.0 Å, similar to those calculated in other CP dimers.[46,47] The computed values are slightly longer than the distances between adjacent nanotube rings determined experimentally by X-ray diffraction for *D,L*-α-SPN (4.7−4.8 Å).[30] To a certain degree, the shorter distances observed experimentally in nanotubes may be a consequence of a synergetic effect that enhances the interaction energies between monomers as the number of units increases. On the basis of B3LYP calculations, Tan et al.[47] predicted this effect on a series of oligomers of *c*-[(β^3-HGly)$_4$-]. Their results have shown a gradual decrease in the average distance between adjacent rings (up to ≈0.1 Å) upon increasing the number of cyclopeptide units.

In the structures investigated in this study, all of the cyclohexane rings exhibit a chair conformation, as expected. In $\alpha-\alpha$OD$_{Acp}$ and $\alpha-\alpha$OD$_{Ach-Acp}$, all of the cyclopentane rings essentially adopt the envelope conformation. However, in the

TABLE 1: Relevant Geometrical Parameters and QTAIM Properties[a] for Dimers of Acp-Based and Ach-Based Cyclic Hexapeptides and Octapeptides[b]

	O···N	O···H	O···H—N	C═O···H	RD[a]	ρ_b(O···H)	$\nabla^2\rho_b$(H—N)	H_b(H—N)	P_b(H—N)[c]
				Hexapeptides					
α−αHD$_{Ach}$	2.985	1.981	167.1	143.9	4.99	0.0223	−1.7910	−0.4954	3.336
α−αHD$_{Acp}$	2.980	1.975	167.5	144.5	4.81	0.0224	−1.7932	−0.4959	3.337
α−αHD$_{Ach-Acp}$	2.974	1.969	167.8	145.2	4.79	0.0226	−1.7932	−0.4959	3.339
γ−γHD$_{Ach}$	2.987	1.987	165.7	157.0	4.86	0.0212	−1.7988	−0.4977	3.309
γ−γHD$_{Acp}$	2.997	2.003	164.2	156.3	4.91	0.0205	−1.8022	−0.4985	3.301
γ−γHD$_{Ach-Acp}$	2.980	1.982	165.8	157.2	4.93	0.0214	−1.8021	−0.4985	3.312
				Octapeptides					
α−αOD$_{Ach}$	2.972	1.970	166.4	144.1	4.97	0.0227	−1.7905	−0.4954	3.335
α−αOD$_{Acp}$	2.976	1.972	167.0	145.4	4.88	0.0224	−1.7944	−0.4962	3.339
α−αOD$_{Ach-Acp}$	2.974	1.971	166.6	145.1	4.92	0.0226	−1.7926	−0.4959	3.337
γ−γOD$_{Ach}$	2.984	1.982	167.2	159.8	4.83	0.0212	−1.8023	−0.4987	3.308
γ−γOD$_{Acp}$	2.953	1.952	166.9	161.5	4.80	0.0226	−1.8088	−0.5002	3.325
γ−γOD$_{Ach-Acp}$	2.965	1.963	166.9	159.5	4.84	0.0221	−1.8029	−0.4987	3.317

[a] Distance between rings. [b] Average distances and angles in Å and degrees, respectively; average values of ρ_b, $\nabla^2\rho_b$, and H_b are given in au. [c] Average position of the bond critical point in the H−N bond (see text).

other dimers containing cyclopentane rings, twist or envelope forms or intermediate conformations are exhibited in the optimized structures. Not surprisingly, the values of the dihedral angles involving cyclopentane ring atoms vary somewhat from ring to ring. This is related to the well-known conformational characteristic of cyclopentane, namely, the pseudorotation, a ring-puckering motion for which computational investigations,[89–91] in agreement with experimental observations,[92–94] predict a nearly free energy barrier.

The distances between N and O atoms intervening in hydrogen bonding are in the range 2.98−2.99 Å in α−αHD$_{Ach}$, 2.94−3.01 Å in α−αHD$_{Acp}$, and 2.95−3.01 Å in α−αHD$_{Ach-Acp}$. The averaged values are collected in Table 1. The interatomic N···O distances determined by X-ray diffraction in the homodimer of *c*-[(*D*-Leu-*L*-^{Me}*N*-γ-Acp)$_3$-] vary from 2.88 to 2.98 Å. These distances are similar to those calculated in this study for the related dimer α−αHD$_{Acp}$. The experimental N···O distances observed in a heterodimer formed by *c*-[(*D*-Leu-*L*-^{Me}*N*-γ-Acp)$_3$-] and *c*-[(*D*-Phe-*L*-^{Me}*N*-γ-Ach)$_3$-] are 2.82−2.90 Å,[25] which are slightly shorter than those observed in the homodimer. This result was used to rationalize the preference for heterodimer formation, considering that the heterodimer is more stable through an improved alignment of the atoms that take part in hydrogen bonding.[25] The average values of the N···O and H···O distances calculated for the α−αHD species follow the experimental trend (see Table 1). To analyze the alignment of the atoms intervening in hydrogen bonding, we considered the O···H—N and C═O···H angles. In principle, the larger the O···H—N angle, the stronger the hydrogen-bonding interaction. For C═O···H angles, if we assume sp^2 hybridization for the carbonyl oxygen, the best alignment would correspond to 120° due to the directionality of the oxygen lone pairs. The average values listed in Table 1 for these angles in the α−αHD structures do not show a clear preference for the heterodimer in terms of favorable geometrical arrangements for stronger hydrogen-bonding interaction.

The O···N and H···O distances in the γ−γHD structures are slightly longer than those in the corresponding α−αHDs. Moreover, in the γ−γHDs, the average C═O···H angles are significantly larger (by ≈10°) and the O···H—N angles are slightly smaller (≈2°) than in the α−α hexapeptide dimers. These results agree with the conclusion, inferred from experimental measurements,[26] that the hydrogen-bond alignment in the α−α pattern is more favorable than that in the γ−γ pattern.

In general, the geometries of the C═O···HN moieties in the α−αODs are very similar among each other (see Table 1). The O···N and O···H distances are about 2.97 and 1.97 Å, respectively, and the O···H—N and C═O···H angles are in the ranges 166−167 and 144−145°, respectively. Unlike the results obtained for the HD species, these geometrical parameters do not show a better alignment for the heterodimer. More differences are exhibited between the different γ−γOD structures. In particular, the Acp-based homodimer has the shortest O···H and O···N distances among all the dimers investigated here (mean values of 1.952 and 2.953 Å, respectively). However, the average C═O···H angle in this structure is the highest (161.5°), and so the least favorable assuming 120° for the ideal alignment. As for the hexapeptide dimers, the C═O···H angles in the α−αOD species (≈145°) are substantially smaller than those in the γ−γODs (values around 160°), which suggests a better hydrogen-bonding alignment for α−α stacking.

As mentioned in the preceding section, we first performed geometry optimizations for monomers employing, as starting points, the geometries they have in the dimers. Subsequently, and in order to search for additional conformers, we carried out canonical MD simulations in chloroform, using for initial conditions the geometries obtained in the previous optimizations. Figure 6 shows the values of the root-mean-square deviations (rmsd's) between the sampled structures and the reference (initial) conformations as a function of time. As can be seen, the MD simulations predict that both α and γ HM$_{Ach}$ structures, as well as αHM$_{Acp}$, are quite stable and rather rigid entities, since the rmsd values are maintained (oscillating around ≈1 Å) along the simulation time. The same happens with αOM$_{Ach}$ and αOM$_{Acp}$; however, in the case of γHM$_{Acp}$, γOM$_{Ach}$, and γOM$_{Acp}$, the rmsd jumps to higher values, suggesting that the starting structures differ significantly from the most stable conformations.

The new structures obtained from the MD trajectories were grouped in clusters according to their rmsd cutoff (in a range from 0.5 to 0.8 Å), and the representative structure for each cluster was used as a starting point for gas-phase geometry optimization at the B3LYP/6-31G(d) level. For the sake of clarity and simplicity, we present in Figures 7−10 only the most relevant conformations of monomers obtained in this study. The geometries (Cartesian coordinates) and energies of all the conformations optimized in this work are presented in the Supporting Information. For γHM$_{Acp}$, we found two relevant

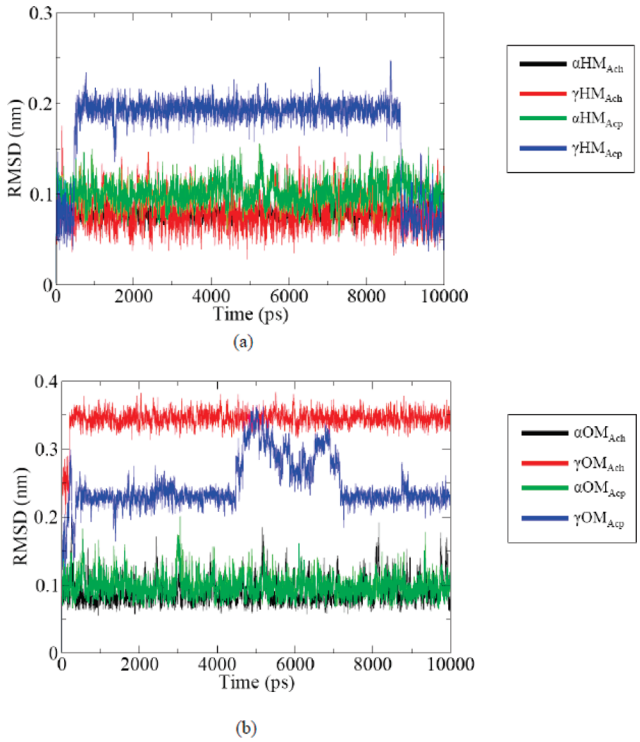

Figure 6. rmsd for the (a) hexameric and (b) octameric monomers during 10 ns of molecular dynamics simulation.

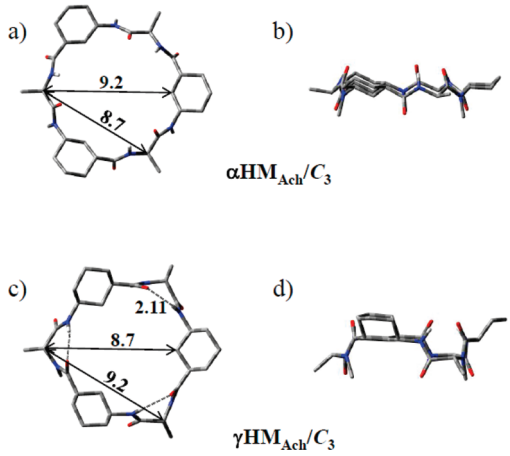

Figure 7. Relevant conformations of αHM_{Ach} and γHM_{Ach} optimized at the B3LYP/6-31G(d) level, as viewed along (a and c) or perpendicular to (b and d) the symmetry axis. The approximate symmetry is indicated. Values for selected interatomic distances are given in Å.

conformations, having C_3 and C_1 symmetry as shown in Figure 8. The single-point B3LYP/6-31+(d,p) calculations predict that the C_3 conformer is slightly more stable (≈1.2 kcal/mol) than the C_1 conformer, but the M05-2X results show that the latter is the most stable conformation by 5.0 kcal/mol. Also, two relevant conformations were obtained for γOM_{Acp}; one has two hydrogen bonds formed between C═O and H—N groups located in front of each other, resembling the β-sheet pattern (see Figure 10), and the other displays a V-shaped structure. The M05-2X calculations predict that the latter structure is more stable than the former by 9.7 kcal/mol, but the B3LYP functional favors the β-sheet-like form by 0.5 kcal/mol. For γOM_{Ach}, we optimized a conformation quite similar to the V-shaped form of γOM_{Acp}; however, the M05-2X calculations predict that it is 4.0 kcal/mol less stable than the β-sheet structure (shown in Figure 9). The lesser stability of the V-shaped form of γOM_{Ach}

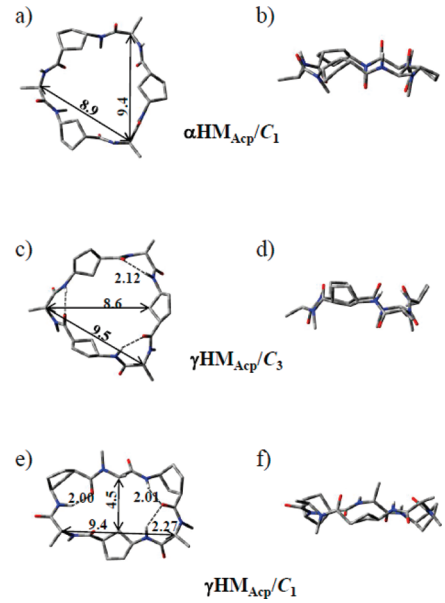

Figure 8. Relevant conformations of αHM_{Acp} and γHM_{Acp} optimized at the B3LYP/6-31G(d) level, as viewed along two different orientations. The approximate symmetry is indicated. Values for selected interatomic distances are given in Å.

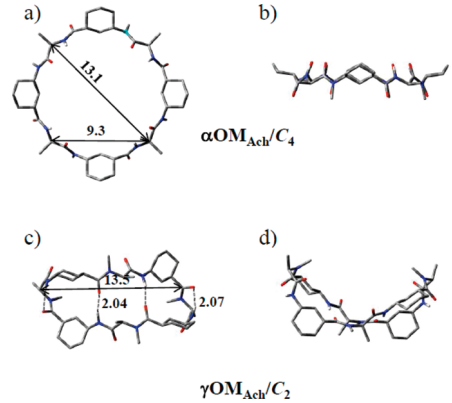

Figure 9. Relevant conformations of αOM_{Ach} and γOM_{Ach} optimized at the B3LYP/6-31G(d) level, as viewed along (a and c) or perpendicular to (b and d) the symmetry axis. The approximate symmetry is indicated. Values for selected interatomic distances are given in Å.

in comparison with the corresponding conformation of γOM_{Acp} may be a result of higher molecular strain because the backbone structure in the former CP involves axial dispositions in the cyclohexane rings.

It is worth noting that γ monomers change the conformation, with respect to that exhibited in the dimer, more extensively than do α monomers. The geometrical changes are especially remarkable for γOM monomers, which show folded conformations, two of them described in the above paragraph. This folding is a result of a balance between conformational stabilization due to formation of intramolecular hydrogen bonds, steric repulsions, and ring flexibility. It may be anticipated that stabilization via intramolecular hydrogen bonding will have a significant influence on the dimerization energies (via an increase in the deformation energies). Although the O···H distances in the α monomers may be within typical distances for hydrogen bonding, the C═O and H—N bonds are almost parallel to each other, which is far away from the most favorable alignment for this kind of interaction.

B. QTAIM Analysis of Hydrogen Bonds. QTAIM has proved to be very useful for investigating general features of

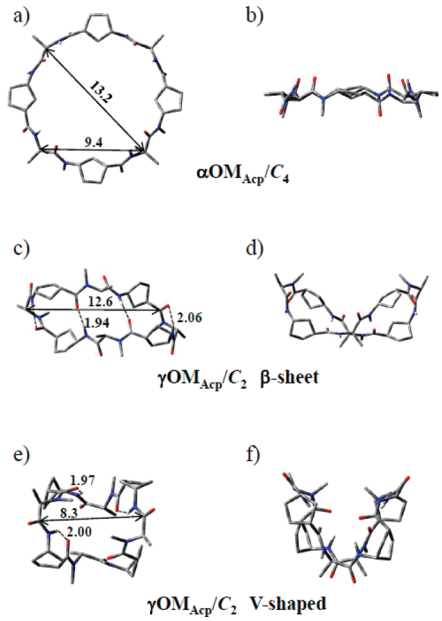

Figure 10. Relevant conformations of αOM$_{Acp}$ and γOM$_{Acp}$ optimized at the B3LYP/6-31G(d) level, as viewed along (a, c, and e) or perpendicular to (b, d, and f) the symmetry axis. The approximate symmetry is indicated. Values for selected interatomic distances are given in Å.

hydrogen bonding.[95–110] It is worth noting that values of the most relevant local properties that can be determined by this theory are almost independent of both basis set and electronic structure method.[110] Good correlation has been found between the interaction energy in hydrogen-bonded systems and the electron density at the bond critical points (ρ_b).[100–110] Correlations between interaction energies and O···H distances have also been reported in the literature;[97,103] therefore, correlations between O···H distances and the corresponding ρ_b may be expected as well, at least from a qualitative point of view. Table 1 includes several local properties calculated at the BCPs of the O···H−N fragments; specifically, ρ_b for the O···H hydrogen bonds and $\nabla^2\rho_b$ and H_b for the H−N bonds. As for the geometrical parameters shown in this table, the figures correspond to mean values in each dimer (detailed results are reported in the Supporting Information). The values of ρ_b collected in Table 1 are typical for strong hydrogen-bonding interaction. As can be seen, good qualitative correlation between O···H distances and ρ_b is found for the HD species. The significant gap between the values of the electron densities calculated for α−αHDs and those obtained for γ−γHDs suggests that hydrogen bonding is stronger in the former species, which agrees with the conclusion derived from experiment. For ODs, however, agreement with the expected correlation is not complete. For example, ρ_b for γ−γOD$_{Acp}$ (0.0226 au) should be larger than that for α−αOD$_{Ach}$ (0.0227 au) because the mean O···H distance in the former is 0.018 Å shorter than in the latter. The reason for this result may be related to the C═O···H−N alignments, which have some influence on ρ_b. Particularly, γ−γOD$_{Acp}$ has one of the less favorable alignments for strong interaction. Notice that, for the Ach-based octameric homodimers, the results of both ρ_b and the geometrical parameters are consistent with stronger hydrogen-bonding interaction for α−α stacking.

As mentioned in the Introduction, it has been suggested, based on experimental measurements, that the H−N group in the α-amino acid is more polarized than that in the γ-amino acid,[26] thus favoring hydrogen bonding in α−α stacking. Although there is not a straightforward way to determine the polarity of a bond in a polyatomic molecule, we tried to investigate this issue with the aid of QTAIM, using several criteria specified as follows. First, we used the position of the BCP, a criterion introduced by Cremer and Kraka[111] to quantitatively measure the polar character of a bond. In this paper, the position of the BCP in the H−N bond, P_b(H−N), is defined as the ratio between the distance of the N atom to the BCP and that of the H atom to the BCP. The closer the BCP is to the H nucleus (i.e., larger values of P_b), the more polar the H−N bond. The mean P_b(H−N) ratios are included in Table 1. The results show a clear displacement of the location of the BCP toward the H nucleus when going from the γ−γ to the α−α dimers, suggesting more polarity of the H−N bonds in the α-amino acids, in agreement with previous conclusions inferred from experimental measurements.[26]

The second criterion is based on the value of $\nabla^2\rho$ at the BCP of the H−N bond. Covalent bonding is characterized by large negative values of $\nabla^2\rho_b$. On the other hand, ionic bonds are characterized by positive values of $\nabla^2\rho_b$.[85] Therefore, the value of $\nabla^2\rho_b$ might be used as a qualitative indicator of the degree of polarization of a bond. As shown in Table 1, there is a noticeable gap between the values of $\nabla^2\rho_b$ for the α−α dimers and those for the γ−γ dimers. The smaller absolute values of the α−α dimers are consistent with larger bond polarization of the H−N groups in the α-amino acids. Likewise, the local density energy evaluated at the BCPs, H_b, has been used to analyze the ionic character of bonds.[111] The ionic character increases with increasing H_b (H_b is positive in ionic bonds). Again, the calculations suggest the H−N bonds of the α-amino acids are more polar than those of the γ-amino acids. Notice that H_b is less sensitive to changes in the electron distribution than is $\nabla^2\rho$.

Finally, it is worth noting that Mulliken charges obtained by single-point B3LYP/6-31+G(d,p) calculations (data listed in the Supporting Information) are also in agreement with the above results. Specifically, the NH groups of the α-amino acids in the α−αHDs show charges around −0.11 au for N and +0.38 au for H, whereas the NH groups of the γ-amino acids in the γ−γHDs present partial charges of ca. +0.09 au for N and +0.37 au for H. Similar results were obtained for the octapeptide dimers.

C. Interaction Energies. The next step in our discussion is concerned with the computed interaction energies, which are collected in Table 2. The single point calculations performed at the B3LYP/6-31+G(d,p) level predict interaction energies around −33 kcal/mol for the three α−α hexapeptide dimers. More accurate interaction energies are, in principle, predicted with the M05-2X functional. With this DFT method, the interaction energies are stronger, especially in the heterodimer (−50.6 kcal/mol). The interaction energy in α−αHD$_{Ach}$ is −49.4 kcal/mol, and that in α−αHD$_{Acp}$ is −49.7 kcal/mol. The interaction energies calculated with B3LYP for the γ−γ hexapeptide dimers are about 2 kcal/mol smaller (in absolute value) than those determined for the corresponding α−α dimers (see Table 2). This agrees with the results on hydrogen bonds described in the preceding sections. Perhaps surprisingly, the interaction energies obtained with the M05-2X functional for the γ−γHD structures are very similar to those computed for the corresponding α−αHD dimers.

In the octapeptide dimers, the B3LYP calculations predict, again, stronger interaction energies for the α−α dimers (ca. −46 kcal/mol) than for the γ−γ dimers (values ranging from −42 to −45 kcal/mol), but the M05-2X calculations favor the γ−γ interaction by 2−5 kcal/mol. These results obtained for the HD

TABLE 2: Interaction and Dimerization Energies (in kcal/mol) for Dimers of Acp-Based and Ach-Based Cyclic Hexapeptides and Octapeptides[a]

	interaction energy		dimerization energy	
	B3LYP	M05-2X	B3LYP	M05-2X
Hexapeptides				
$\alpha-\alpha HD_{Ach}$	−32.9 (3.4)	−49.4 (3.4)	−23.6	−40.0
$\alpha-\alpha HD_{Acp}$	−33.7 (3.5)	−49.7 (3.4)	−30.1	−41.4
$\alpha-\alpha HD_{Ach-Acp}$	−33.4 (3.4)	−50.6 (3.5)	−27.0	−42.2
$\gamma-\gamma HD_{Ach}$	−31.0 (3.7)	−49.7 (3.8)	−14.5	−25.8
$\gamma-\gamma HD_{Acp}$	−30.6 (3.4)	−49.4 (3.4)	−8.1[b]	−8.2[c]
$\gamma-\gamma HD_{Ach-Acp}$	−31.0 (3.6)	−51.0 (3.6)	−12.8[b]	−20.5[c]
Octapeptides				
$\alpha-\alpha OD_{Ach}$	−46.1 (4.6)	−67.8 (4.7)	−19.4	−39.8
$\alpha-\alpha OD_{Acp}$	−46.5 (4.3)	−66.1 (4.3)	−32.6	−50.4
$\alpha-\alpha OD_{Ach-Acp}$	−46.2 (4.5)	−66.7[d]	−26.4	−45.3[d]
$\gamma-\gamma OD_{Ach}$	−44.0 (4.7)	−70.0 (4.8)	−16.9	−15.5
$\gamma-\gamma OD_{Acp}$	−41.7 (4.6)	−70.8 (4.6)	−13.4[e]	+5.9[f]
$\gamma-\gamma OD_{Ach-Acp}$	−44.9 (4.6)	−72.0[d]	−14.8[e]	−3.9[d,f]

[a] Single point calculations with the 6-31+G(d,p) basis set at the B3LYP/6-31G(d) optimized geometries. The energies were corrected for BSSE (values in parentheses). [b] Considering the C_3 conformation of γHM_{Acp}. [c] Considering the C_1 conformation of γHM_{Acp}. [d] BSSE was taken from the B3LYP computations because of SCF convergence failure in the counterpoise calculation. [e] Considering the β-sheet type form of γOM_{Acp}. [f] Considering the V-shaped structure of γOM_{Acp}.

TABLE 3: Deformation Energies (in kcal/mol) Taking Place upon Dimerization of Acp-Based and Ach-Based Cyclic Hexapeptides and Octapeptides[a]

	B3LYP	M05−2X
Hexapeptides		
αHM_{Ach} in $\alpha-\alpha HD_{Ach}$	4.7	4.7
αHM_{Acp} in $\alpha-\alpha HD_{Acp}$	1.8	4.1
αHM_{Ach} in $\alpha-\alpha HD_{Ach-Acp}$	4.6	5.3
αHM_{Acp} in $\alpha-\alpha HD_{Ach-Acp}$	1.8	3.1
γHM_{Ach} in $\gamma-\gamma HD_{Ach}$	8.3	12.0
γHM_{Acp} in $\gamma-\gamma HD_{Acp}$	11.3[b]	20.6[c]
γHM_{Ach} in $\gamma-\gamma HD_{Ach-Acp}$	8.6	11.7
γHM_{Acp} in $\gamma-\gamma HD_{Ach-Acp}$	9.6[b]	18.8[c]
Octapeptides		
αOM_{Ach} in $\alpha-\alpha OD_{Ach}$	13.3	14.0
αOM_{Acp} in $\alpha-\alpha OD_{Acp}$	7.0	7.8
αOD_{Ach} in $\alpha-\alpha OD_{Ach-Acp}$	12.8	13.5
αOD_{Acp} in $\alpha-\alpha OD_{Ach-Acp}$	7.1	8.0
γOM_{Ach} in $\gamma-\gamma OD_{Ach}$	13.6	27.2
γOM_{Acp} in $\gamma-\gamma OD_{Acp}$	15.5[d]	38.4[e]
γOM_{Ach} in $\gamma-\gamma OD_{Ach-Acp}$	13.2	26.8
γOM_{Acp} in $\gamma-\gamma OD_{Ach-Acp}$	16.9[d]	41.3[e]

[a] Single point calculations with the 6-31+G(d,p) basis set at the B3LYP/6-31G(d) optimized geometries. [b] Considering the C_3 conformation of γHM_{Acp}. [c] Considering the C_1 conformation of γHM_{Acp}. [d] Considering the β-sheet form of γOM_{Acp}. [e] Considering the V-shaped structure of γOM_{Acp}.

and OD species suggest that the strengths of the interaction energies in the $\gamma-\gamma$ structures are rather similar to those in the $\alpha-\alpha$ structures. At first glance, this may appear to contradict the above conclusion of stronger hydrogen bonding in the $\alpha-\alpha$ dimers (with the exception of Acp-based ODs), but we notice that van der Waals interactions in these systems may be significant and may vary somewhat in the $\alpha-\alpha$ and $\gamma-\gamma$ patterns (in general, from dimer to dimer).

In previous studies on related compounds,[42,47] approximate strengths of hydrogen bonds were estimated by assuming that all of the interaction energy between the CP rings (this includes hydrogen bonding and van der Waals interactions) is associated with hydrogen bonding only. This assumption is, obviously, an oversimplification because, as already noticed, the van der Waals interactions may be important in these systems. However, for comparison purposes only, we have followed this approximation and estimated average values for each ternary group having the same binding pattern ($\alpha-\alpha$ or $\gamma-\gamma$). The B3LYP calculations for the $\alpha-\alpha$HD group predict an interaction energy of −5.6 kcal/mol per hydrogen bond, whereas M05-2X gives −8.3 kcal/mol. For the $\gamma-\gamma$HD species, the above functionals predict −5.1 and −8.3 kcal/mol, respectively. For $\alpha-\alpha$OD, the average interaction energies per hydrogen bond are −5.8 and −8.4 kcal/mol, respectively, and for $\gamma-\gamma$OD, −5.4 and −8.9 kcal/mol, respectively. Our B3LYP values are very similar to that calculated for *c*-[(*L*-Phe[1]-*D*-Ala[2])$_4$] using the same functional (−5.7 kcal/mol), as expected.[46] The M05-2X results are close to the average interaction energy per hydrogen bond calculated by Lewis and co-workers[42] for *c*-[(*D*-Ala-*L*-Glu-*D*-Ala-*L*-Gln)$_{m=1-4}$], −7.3 kcal/mol, using a hybrid theoretical method in which intermolecular interactions (e.g., hydrogen bonds) are treated with a simple theory that accounts for Coulombic, exchange, and hopping interactions between the weakly interacting fragments. The present calculations support the reliability of their theoretical approach. Finally, it is worth mentioning that the energies per hydrogen bond reported in the experimental studies on hexapeptides and octapeptides are very small (less than 1 kcal/mol) compared with the above values.[26] We notice that the experimental estimates were obtained from standard enthalpies of dimerization, which include additional terms such as deformation energies of the monomers and interactions with the solvent. Therefore, they may underestimate significantly the strength of the hydrogen bonds in the CP dimers.

D. Dimerization Energies. In the preceding section, we have seen that the calculated strength of $\gamma-\gamma$ hydrogen bonds is very similar to that of $\alpha-\alpha$ hydrogen bonds. If this was to be the case, how could we explain the experimental observation that the association constants for $\alpha-\alpha$ dimerization are considerably larger than those for $\gamma-\gamma$ dimerization? The answer to this question can be readily obtained by analyzing the differences in the dimerization energies. In fact, to make a comparison of energetic stabilities of CP dimers, one should use dimerization energies rather than interaction energies. The dimerization energies take into account that, when the monomers separate from the dimer, their geometries may relax so as to acquire a more stable conformation. The energy involved in this conformational relaxation, in absolute value, is called the deformation energy. In other words, the deformation energy is the energy required to distort the conformations of the isolated monomers in order to reach the configurations they have in the dimer.

The dimerization energies calculated in the gas phase are presented in Table 2. As can be seen, the dimerization energies of the $\alpha-\alpha$ dimers are substantially higher, in absolute value, than those of the $\gamma-\gamma$ dimers; this indicates that $\alpha-\alpha$ stacking is clearly favored over $\gamma-\gamma$ stacking. Specifically, the average dimerization energies obtained for the $\alpha-\alpha$HD group are −27 (B3LYP) and −41 kcal/mol (M05-2X), whereas those for $\gamma-\gamma$HDs are −12 (B3LYP) and −18 kcal/mol (M05-2X). The average dimerization energies for $\alpha-\alpha$ODs are −26 (B3LYP) and −45 kcal/mol (M05-2X), and those for $\gamma-\gamma$ODs are −15 (B3LYP) and −4.5 kcal/mol (M05-2X). As we anticipated in a previous section, the reason for this trend arises from the higher stabilization of the γ monomers due to intramolecular hydrogen bonding, which leads to an increase in the deformation energies. Thus, as shown in Table 3, the deformation energies for α monomers are, in general, significantly lower than those

calculated for γ monomers, especially when the M05-2X functional is employed. The results obtained with this functional suggest that formation of γ−γOD$_{Acp}$, which has a positive dimerization energy, is not thermodynamically favorable (notice that dimerization is always entropically unfavorable).

As mentioned in the Introduction, experimental work with hexameric and octameric CPs showed that α−α heterodimerization is strongly preferred over α−α homodimerization. Specifically, in a (0.8:1) mixture of *c*-[(*D*-Leu-*L*-^{Me}*N*-γ-Acp)$_3$-] and *c*-[(*D*-Phe-*L*-^{Me}*N*-γ-Ach)$_3$-] at 298 K, the heterodimer is about 30 times more abundant than the homodimer. The dimerization energies reported in Table 2 for the α−α dimers are consistent with an energetic preference for heterodimerization. For example, formation of 2 mol of α−αHD$_{Ach-Acp}$ is energetically favored over formation of 1 mol of α−αHD$_{Ach}$ and 1 mol of α−αHD$_{Acp}$ by 0.3 (B3LYP) or 3.0 kcal/mol (M05-2X). However, we notice that these energy differences are smaller than the errors associated with the level of theory employed and so this result should be taken with care. Moreover, a more rigorous treatment of this issue would involve the calculation of free energies, but unfortunately frequency calculations at the B3LYP/6-31G(d) level are computationally unaffordable due to the size of the systems that are being investigated here. Also, it would be desirable to evaluate the influence of the solvent on the dimerization energies in order to make a more appropriate comparison with experiment. However, the available continuum solvation models are not well adapted for describing the solvation phenomena of these large systems, and therefore we do not present this type of calculations in this study. Particularly, single-point B3LYP/6-31+G(d,p) calculations with the polarizable continuum model (PCM),[112–115] using chloroform as a solvent, predict that the solvation free energies in these systems are not dominated by long-range interactions (mainly electrostatic + polarization contributions) but rather by short-range and specific interactions, mainly associated to large dispersion and cavitation contributions. This is the expected consequence of dealing with large-size molecules of low polarity in poor polar solvents.

IV. Conclusions

DFT calculations were performed to characterize the molecular structures of model dimers of hexameric and octameric γ-Ach-based and γ-Acp-based α,γ-cyclopeptides, which constitute the building blocks of a promising class of self-assembling nanotubes, and to investigate the origin of the marked difference between α−α and γ−γ association constants, as well as the observed preference for α−α heterodimerization. Full geometry optimizations were done at the B3LYP/6-31G(d) level, and single point calculations with the B3LYP and M05-2X functionals and the 6-31+G(d,p) basis set were then carried out to improve the energetics.

In general, the conformations of the dimers resemble the crystallographic structures of related compounds determined by X-ray diffraction. The analysis of geometrical parameters and local properties of the electron density that characterize the intermolecular hydrogen bonds in these compounds suggest that, in the hexapeptide dimers, hydrogen-bonding interactions are stronger in the α−α stacking, in agreement with the experimental interpretation. This is also found when we compare the results of α−αOD$_{Ach}$ and γ−γOD$_{Ach}$, but discrepancies are apparent for Acp-based ODs. The calculations corroborate previous suggestions, inferred from experimental measurements,[26] that the NH groups of the α-amino acids are more polarized than those of the γ-amino acids. The calculations reveal that γ monomers may adopt conformations with intramolecular hydrogen bonds, a feature that is not present in the α monomers. This has significant implications in the relative stabilities of α−α and γ−γ dimers.

The B3LYP interaction energies predicted for the α−α dimers are slightly stronger (by ≈2 kcal/mol) than those determined for the γ−γ species. However, the M05-2X functional gives almost the same interaction energies for both the α−αHD and γ−γHD species, and the interaction energies calculated with this functional for the γ−γODs are somewhat higher, in absolute value, than those obtained for the α−αODs (by 2−5 kcal/mol). These results suggest that the strength of α−α stacking (due to hydrogen-bonding and van der Waals interactions) is rather similar to that of γ−γ stacking.

The dimerization energies calculated with the B3LYP and M05-2X functionals show a clear preference for the α−α hydrogen-bonding pattern. The stabilization of the γ monomers due to intramolecular hydrogen bonding results in a significant increase of the deformation energies in this type of monomers, which in turn leads to a decrease, in absolute value, of the dimerization energies. Finally, the calculations predict that α−α heterodimerization is energetically favored over α−α homodimerization, although the energy differences accompanying hetero- and homodimerization are very similar to each other. Entropic contributions, not explored in this study, may also play a significant role in this type of dimerization processes.

Acknowledgment. This work was supported by Spanish Ministry of Education and Science and the ERDF [SAF2007-61015 and Consolider Ingenio 2010 (CSD2007-00006)], and Xunta de Galicia (GRC2006/132, 2009/029, GRC2007/50, PGIDIT08CSA047209PR, and PGIDIT07PXIB209072PR). The authors thank "Centro de Supercomputación de Galicia (CESGA)" for the use of their computational resources. We are very grateful for helpful discussions with Prof. Enrique Sanchez Marcos and Prof. Ricardo A. Mosquera. R.G.-F. thanks Xunta de Galicia (programa Ángeles Alvariño) and Ministerio de Ciencia e Innovación (programa José Castillejo) for fellowships.

Supporting Information Available: Tables showing geometries (Cartesian coordinates) and energies of all of the conformations optimized in this work, as well as QTAIM properties and Mulliken charges obtained by single-point B3LYP/6-31+G(d,p) calculations. This material is available free of charge via the Internet at http://pubs.acs.org.

References and Notes

(1) Iijima, S. *Nature* **1991**, *354*, 56.
(2) Iijima, S.; Ichihashi, T. *Nature* **1993**, *363*, 603.
(3) Postma, H. W. C.; Teepen, T.; Yao, Z.; Grifoni, M.; Dekker, C. *Science* **2001**, *293*, 76.
(4) Bong, D. T.; Clark, T. D.; Granja, J. R.; Ghadiri, M. R. *Angew. Chem., Int. Ed.* **2001**, *40*, 988.
(5) Patzke, G. R.; Krumeich, F.; Nesper, R. *Angew. Chem., Int. Ed.* **2002**, *41*, 2446.
(6) Gudiksen, M. S.; Wang, J.; Lieber, C. M. *J. Phys. Chem. B* **2001**, *105*, 4062.
(7) Lauhon, L. J.; Gudiksen, M. S.; Wang, D.; Lieber, C. M. *Nature* **2002**, *420*, 57.
(8) Xia, Y.; Yang, P.; Sun, Y.; Wu, Y.; Mayers, B.; Gates, B.; Yin, Y.; Kim, F.; Yan, H. *Adv. Mater.* **2003**, *15*, 353.
(9) Qian, C.; Kim, F.; Ma, L.; Tsui, F.; Yang, P.; Liu, J. *J. Am. Chem. Soc.* **2004**, *126*, 1195.
(10) Krausch, G.; Magerle, R. *Adv. Mater.* **2002**, *14*, 1579.
(11) Lazzari, M.; López-Quintela, M. A. *Adv. Mater.* **2003**, *15*, 1583.
(12) Murray, C. B.; Sun, S.; Gaschler, W.; Doyle, H.; Betley, T. A.; Kagan, C. R. *IBM J. Res. Dev.* **2001**, *45*, 47.
(13) Love, J. C.; Estroff, L. A.; Kriebel, J. K.; Nuzzo, R. G.; Whitesides, G. M. *Chem. Rev.* **2005**, *105*, 1103.

(14) Ghadiri, M. R.; Granja, J. R.; Milligan, R. A.; McRee, D. E.; Khazanovich, N. *Nature* **1993**, *366*, 324.
(15) Brea, R. J.; Reiriz, C.; Granja, J. R. *Chem. Soc. Rev.* DOI: 10.1039/B805753M.
(16) Seebach, D.; Matthews, J. L.; Meden, A.; Wessels, T.; Baerlocher, C.; McCusker, L. B. *Helv. Chim. Acta* **1997**, *80*, 173.
(17) Karle, I. L.; Handa, B. K.; Hassall, C. H. *Acta Crystallogr., Sect. B* **1975**, *31*, 555.
(18) Leclair, S.; Baillargeon, P.; Skouta, R.; Gauthier, D.; Zhao, Y.; Dory, Y. L. *Angew. Chem., Int. Ed.* **2004**, *43*, 349.
(19) Horne, W. S.; Stout, C. D.; Ghadiri, M. R. *J. Am. Chem. Soc.* **2003**, *125*, 9372.
(20) Ranganathan, D.; Lakshmi, C.; Karle, I. L. *J. Am. Chem. Soc.* **1999**, *121*, 6103.
(21) Semetey, V.; Didierjean, C.; Briand, J. P.; Aubry, A.; Guichard, G. *Angew. Chem., Int. Ed.* **2002**, *41*, 1895.
(22) Shimizu, L. S.; Hughes, A. D.; Smith, M. D.; Davis, M. J.; Zhang, B. P.; Loye, H.-C.; Shimizu, K. D. *J. Am. Chem. Soc.* **2003**, *125*, 14972.
(23) Brea, R. J.; Castedo, L.; Granja, J. R. *Chem. Commun.* **2007**, 3267.
(24) Amorin, M.; Castedo, L.; Granja, J. R. *J. Am. Chem. Soc.* **2003**, *125*, 2844.
(25) Brea, R. J.; Amorín, M.; Castedo, L.; Granja, J. R. *Angew. Chem., Int. Ed.* **2005**, *44*, 5710.
(26) Amorín, M.; Castedo, L.; Granja, R. J. *Chem.—Eur. J.* **2005**, *11*, 6543.
(27) For the sake of simplicity, the (italic) letter *D* is used to denote the (1*R*,3*S*) isomer and the letter *L* is used to name the (1*S*,3*R*) isomer.
(28) Brea, R. J.; Vázquez, M. E.; Mosquera, M.; Castedo, L.; Granja, J. R. *J. Am. Chem. Soc.* **2007**, *129*, 1653.
(29) Amorín, M.; Castedo, L.; Granja, J. R. *Chem.—Eur. J.* **2008**, *14*, 2100.
(30) Hartgerink, J. D.; Granja, J. R.; Milligan, R. A.; Ghadiri, M. R. *J. Am. Chem. Soc.* **1996**, *118*, 43.
(31) Khazanovich, N.; Granja, J. R.; McRee, D. E.; R. A. Milligan, R. A.; Ghadiri, M. R. *J. Am. Chem. Soc.* **1994**, *116*, 6011.
(32) Clark, T. D.; Buriak, J. M.; Kobayashi, K.; Isler, M. P.; McRee, D. E.; Ghadiri, M. R. *J. Am. Chem. Soc.* **1998**, *120*, 8949.
(33) Ghadiri, M. R.; Granja, J. R.; Buehler, L. K. *Nature* **1994**, *369*, 301.
(34) Granja, J. R.; Ghadiri, M. R. *J. Am. Chem. Soc.* **1994**, *116*, 10785.
(35) Sanchez-Quesada, J.; Kim, H. S.; Ghadiri, M. R. *Angew. Chem., Int. Ed.* **2001**, *40*, 2503.
(36) Reiriz, C.; Amorín, M.; García-Fandiño, R.; Castedo, L.; Granja, J. R. *Org. Biomol. Chem.* **2009**, *7*, 4358.
(37) García-Fandiño, R.; Granja, J. R.; Marco, D. A.; Orozco, M. *J. Am. Chem. Soc.* **2009**, *131*, 15678.
(38) Möhle, D.; Hofman, H.-J. *J. Pept. Res.* **1998**, *51*, 19.
(39) Vitoux, B.; Aubry, A.; Cung, M. T.; Marraud, M. *Int. J. Pept. Protein Res.* **1986**, *27*, 617.
(40) Brea, R. J.; Castedo, L.; Granja, J. R.; Herranz, M. Á.; Sanchez, L.; Martín, N.; Seitz, W.; Guldi, D. M. *Proc. Natl. Acad. Sci. U.S.A.* **2007**, *104*, 5291.
(41) Gailer, C.; Figel, M. *J. Comput.-Aided Mol. Des.* **1997**, *11*, 273.
(42) Lewis, J. P.; Pawley, N. H.; Sankey, O. F. *J. Chem. Phys. B* **1997**, *101*, 10576.
(43) Carloni, P.; Andreoni, W.; Parrinello, M. *Phys. Rev. Lett.* **1997**, *79*, 761.
(44) Jishi, R. A.; Flores, R. M.; Valderrama, M.; Lou, L.; Bragin, J. *J. Phys. Chem. A* **1998**, *102*, 9858.
(45) Jishi, R. A.; Braier, N. C.; White, C. T.; Mintmire, J. W. *Phys. Rev. B* **1998**, *58*, R16009.
(46) Chen, G.; Su, S.; Liu, R. *J. Phys. Chem. B* **2002**, *106*, 1570.
(47) Tan, H.; Qu, W.; Chen, G.; Liu, R. *Chem. Phys. Lett.* **2003**, *369*, 556.
(48) Okamoto, H.; Takeda, K.; Shiraishi, K. *Phys. Rev. B* **2001**, *64*, 115425.
(49) Okamoto, H.; Nakanishi, T.; Nagai, Y.; Kasahara, M.; Takeda, K. *J. Am. Chem. Soc.* **2003**, *125*, 2756.
(50) de Brito Mota, F.; Rivelino, R. *THEOCHEM* **2006**, *776*, 53.
(51) Takahashi, R.; Wang, H.; Lewis, J. P. *J. Phys. Chem. B* **2007**, *111*, 9093.
(52) Kihara, S.; Takagi, H.; Takechi, K.; Takeda, K. *J. Phys. Chem. B* **2008**, *112*, 7631.
(53) Engels, M.; Bashford, D.; Ghadiri, M. R. *J. Am. Chem. Soc.* **1995**, *117*, 9151.
(54) Asthagiri, D.; Bashford, D. *Biophys. J.* **2002**, *82*, 1176.
(55) Tarek, M.; Maigret, B.; Chipot, C. *Biophys. J.* **2003**, *85*, 2287.
(56) Pan, Y.; Birkedal, H.; Pattison, P.; Brown, D.; Chapuis, G. *J. Phys. Chem. B* **2004**, *108*, 6458.
(57) Hwang, H.; Schatz, G. C.; Ratner, M. A. *J. Phys. Chem. A* **2009**, *113* (16), 4780–4787.
(58) Khurana, E.; Nielsen, S. O.; Ensing, B.; Klein, M. L. *J. Phys. Chem. B* **2006**, *110*, 18965.
(59) Cheng, J.; Zhu, J.; Liu, B. *Chem. Phys.* **2007**, *333*, 105.
(60) Praveena, G.; Kolandaivel, P.; Santhanamoorthi, N.; Renugopalakrishnan, V.; Ramakrishna, S. *J. Nanosci. Nonotechnol.* **2007**, *7*, 2253.
(61) Praveena, G.; Kolandaivel, P. *THEOCHEM* **2009**, *900*, 96.
(62) Praveena, G.; Kolandaivel, P. *J. Mol. Model.* **2008**, *14*, 1147.
(63) Santhanamoorthi, N.; Kolandaivel, P.; Renugopalakrishnan, V.; Ramakrishna, S. *J. Comput. Theor. Nanosci.* **2008**, *5*, 2264.
(64) Kolandaivel, P.; Abiram, A. *Mol. Simul.* **2009**, *35*, 409.
(65) Santhanamoorthi, N.; Kolandaivel, P.; Senthilkumar, K. *J. Mol. Graphics Modell.* **2009**, *27*, 784.
(66) De Santis, P.; Morosetti, S.; Rizzo, R. *Macromolecules* **1974**, *7*, 52.
(67) Kobayashi, K.; Granja, J. R.; Ghadiri, M. R. *Angew. Chem., Int. Ed.* **1995**, *34*, 95.
(68) Becke, A. D. *J. Chem. Phys.* **1992**, *96*, 2155.
(69) Becke, A. D. *J. Chem. Phys.* **1993**, *98*, 5648.
(70) Lee, C.; Yang, W.; Parr, R. G. *Phys. Rev. B* **1988**, *37*, 785.
(71) Zhao, Y.; Schultz, N. E.; Truhlar, D. G. *J. Chem. Theory Comput.* **2006**, *2*, 364.
(72) Zhao, Y.; Truhlar, D. G. *J. Chem. Theory Comput.* **2007**, *3*, 289.
(73) Jurecka, P.; Sponer, J.; Cerny, J.; Hobza, P. *Phys. Chem. Chem. Phys.* **2006**, *8*, 1985.
(74) Hehre, W. J.; Radom, L.; Schleyer, P. v. R.; Pople, J. A. *Ab Initio Molecular Orbital Theory*, 1st ed.; Wiley: New York, 1986.
(75) Frisch, M. J.; Trucks, G. W.; Schlegel, H. B.; Scuseria, G. E.; Robb, M. A.; Cheeseman, J. R.; Montgomery, J. A., Jr.; Vreven, T.; Kudin, K. N.; Burant, J. C.; Millam, J. M.; Iyengar, S. S.; Tomasi, J.; Barone, V.; Mennucci, B.; Cossi, M.; Scalmani, G.; Rega, N.; Petersson, G. A.; Nakatsuji, H.; Hada, M.; Ehara, M.; Toyota, K.; Fukuda, R.; Hasegawa, J.; Ishida, M.; Nakajima, T.; Honda, Y.; Kitao, O.; Nakai, H.; Klene, M.; Li, X.; Knox, J. E.; Hratchian, H. P.; Cross, J. B.; Bakken, V.; Adamo, C.; Jaramillo, J.; Gomperts, R.; Stratmann, R. E.; Yazyev, O.; Austin, A. J.; Cammi, R.; Pomelli, C.; Ochterski, J. W.; Ayala, P. Y.; Morokuma, K.; Voth, G. A.; Salvador, P.; Dannenberg, J. J.; Zakrzewski, V. G.; Dapprich, S.; Daniels, A. D.; Strain, M. C.; Farkas, O.; Malick, D. K.; Rabuck, A. D.; Raghavachari, K.; Foresman, J. B.; Ortiz, J. V.; Cui, Q.; Baboul, A. G.; Clifford, S.; Cioslowski, J.; Stefanov, B. B.; Liu, G.; Liashenko, A.; Piskorz, P.; Komaromi, I.; Martin, R. L.; Fox, D. J.; Keith, T.; Al-Laham, M. A.; Peng, C. Y.; Nanayakkara, A.; Challacombe, M.; Gill, P. M. W.; Johnson, B.; Chen, W.; Wong, M. W.; Gonzalez, C.; Pople, J. A. *Gaussian 03*, revision E.01; Gaussian, Inc.: Wallingford, CT, 2004.
(76) Boys, S. F.; Bernardi, F. *Mol. Phys.* **1970**, *19*, 553.
(77) Simon, S.; Duran, M.; Dannenberg, J. J. *J. Chem. Phys.* **1996**, *105*, 11024.
(78) Hess, B.; Kutzner, C.; van der Spoel, D.; Lindahl, E. *J. Chem. Theory Comput.* **2008**, *4*, 435.
(79) Wang, J.; Wang, W.; Kollman, P. A.; Case, D. A. *J. Mol. Graphics Modell.* **2006**, *25*, 247260.
(80) Wang, J.; Wolf, R. M.; Caldwell, J. W.; Kollman, P. A.; Case, D. A. *J. Comput. Chem.* **2004**, *25*, 1157.
(81) Fox, T.; Kollman, P. A. *J. Phys. Chem. B* **1998**, *102*, 8070.
(82) Cieplak, P.; Caldwell, J. W.; Kollman, P. A. *J. Comput. Chem.* **2001**, *22*, 1048.
(83) Hess, B.; Bekker, H.; Berendsen, H. J. C.; Fraaije, J. G. E. M. *J. Comput. Chem.* **1997**, *18*, 1463.
(84) Essman, U.; Perera, L.; Berkowitz, M.; Darden, T.; Lee, H.; Pedersen, L. *J. Chem. Phys.* **1995**, *103*, 8577.
(85) Bader, R. F. W. *Atoms in Molecules: A Quantum Theory*; Oxford University Press: Oxford, U.K., 1990.
(86) Bader, R. F. W. *Chem. Rev.* **1991**, *91*, 893.
(87) *AIMPAC: A suite of programs for the Theory of Atoms in Molecules*; Bader, R. W. F., and co-workers, Eds.; McMaster University: Hamilton, Ontario, Canada.
(88) Biegler-König, F. W.; Bader, R. F. W.; Tang, T.-H. *J. Comput. Chem.* **1982**, *3*, 317.
(89) Cremer, D.; Pople, J. A. *J. Am. Chem. Soc.* **1975**, *97*, 1358.
(90) Han, S. J.; Kang, Y. K. *THEOCHEM* **1996**, *362*, 243.
(91) Wu, A.; Cremer, D.; Auer, A. A.; Gauss, J. *J. Phys. Chem. A* **2002**, *106*, 657.
(92) Adams, W. J.; Geise, H. J.; Bartell, L. S. *J. Am. Chem. Soc.* **1970**, *92*, 5013.
(93) Carreira, L. A.; Jiang, G. J.; Person, W. B.; Willis, J. J. N. *J. Chem. Phys.* **1972**, *56*, 1440.
(94) Bauman, L. E.; Laane, J. *J. Chem. Phys.* **1988**, *92*, 1040.
(95) Mo, O.; Yanez, M.; Elguero, J. *J. Chem. Phys.* **1992**, *97*, 6628.
(96) Mó, O.; Yáñez, M.; Elguero, J. *THEOCHEM* **1994**, *314*, 73.
(97) Espinosa, E.; Molins, E.; Lecomte, C. *Chem. Phys. Lett.* **1998**, *285*, 170.
(98) Gatti, C.; Saunders, V. R.; Roetti, C. *J. Chem. Phys.* **1994**, *101*, 10686.
(99) Palusiak, M.; Grabowski, S. J. *J. Mol. Struct.* **2002**, *642*, 97.
(100) Koch, U.; Popelier, P. L. A. *J. Chem. Phys.* **1995**, *99*, 9747.
(101) Grabowski, S. J. *J. Phys. Chem. A* **2000**, *104*, 5551.

(102) Grabowski, S. J. *J. Phys. Chem. A* **2001**, *105*, 10739.
(103) Grabowski, S. J. *J. Mol. Struct.* **2001**, *562*, 137.
(104) Parthasarathi, R.; Amutha, R.; Subramanian, V.; Nair, B. U.; Ramasami, T. *J. Phys. Chem. A* **2004**, *108*, 3817.
(105) Parthasarathi, R.; Subramanian, V.; Sathyamurthy, N. *J. Phys. Chem. A* **2005**, *109*, 843.
(106) Parthasarathi, R.; Subramanian, V.; Sathyamurthy, N. *J. Phys. Chem. A* **2006**, *110*, 3349.
(107) Parthasarathi, R.; Raman, S. S.; Subramanian, V.; Ramasami, T. *J. Phys. Chem. A* **2007**, *111*, 7141.
(108) Boyd, R. J.; Choi, S. C. *Chem. Phys. Lett.* **1985**, *120*, 80.
(109) Boyd, R. J.; Choi, S. C. *Chem. Phys. Lett.* **1986**, *129*, 62.
(110) Jablonski, M.; Palusiak, M. *J. Phys. Chem. A* **2010**, *114*, 2240.
(111) Cremer, D.; Kraka, E. *Croat. Chem. Acta* **1984**, *57*, 1259.
(112) Cances, E.; Mennucci, B.; Tomasi, J. *J. Chem. Phys.* **1997**, *107*, 3032.
(113) Mennucci, B.; Tomasi, J. *J. Chem. Phys.* **1997**, *106*, 5151.
(114) Cossi, M.; Barone, V.; Mennucci, B.; Tomasi, J. *Chem. Phys. Lett.* **1998**, *286*, 253.
(115) Cossi, M.; Scalmani, G.; Rega, N.; Barone, V. *J. Chem. Phys.* **2002**, *117*, 43.

JP910919K